JOURNAL OF AGRICULTURAL AND FOOD CHEMISTRY

J. Agric. Food Chem. **2003,** *51,* 7951−7961 **7951**

Reactions of Anthocyanins and Tannins in Model Solutions

ERIKA SALAS,* HÉLÈNE FULCRAND, EMMANUELLE MEUDEC, AND VÉRONIQUE CHEYNIER

INRA-UMR Sciences pour l'Œnologie, Equipe SSIP, 2 Place Viala, 34060 Montpellier, France

The reaction between procyanidin dimer Ec-EcG (B2 3′-*O*-gallate) and malvidin 3-*O*-glucoside (Mv3glc) was studied in a model solution system at two different pH values, 2.0 and 3.8. Disappearance of both species was much faster at pH 3.8 than at pH 2.0. That of Mv3glc was increased in the presence of Ec-EcG, whereas that of Ec-EcG was the same in the presence or absence of the anthocyanin. Values of absorbance at 520 nm measured at pH 2.0 were correlated with the amount of residual Mv3glc. Those measured at pH 3.8 hardly changed during the incubation, but absorbance values at 420 and 620 nm as well as resistance to sulfite bleaching were much increased, confirming that Mv3glc was converted to other pigments. Anthocyanin−flavanol adducts were observed at both pH values, but their structures were different. At pH 2.0, cleavage of the procyanidin linkage followed by nucleophilic addition of flavanol or anthocyanin moieties led to $(Ec)_n$-EcG and $(Ec)_n$-Mv3glc, respectively. At pH 3.8, nucleophilic addition of Ec-EcG onto the anthocyanin yielded Mv3glc-(Ec-EcG).

KEYWORDS: Anthocyanins; malvidin 3-glucoside; flavanols; procyanidins; adducts; LC-ESI/MS; MS-MS; derived pigments

INTRODUCTION

Red wine is rich in phenolic compounds, which are responsible for its color and astringency and also contribute to its flavor. During aging and storage of red wine, many changes occur. Anthocyanins, which are the red grape pigments and responsible for the color of young red wines, are slowly converted into new pigments by condensation with other phenolic compounds such as flavanols during wine storage. These new pigments are more resistant to decolorization by sulfur dioxide than their anthocyanin precursors (*1*) and present different color properties.

Two major ways for anthocyanin−flavanol reaction, namely, acetaldehyde-mediated condensation and direct tannin anthocyanin addition, are reported. Acetaldehyde, resulting from ethanol oxidation or produced by yeast metabolism, is naturally present in wine. Condensation of malvidin 3-*O*-glucoside and flavanols (catechin or epicatechin) via an ethyl bridge arising from acetaldehyde was demonstrated in both model solutions and wine (*2*−*4*). Recently, the existence of an ethyl-linked malvidin 3-*O*-glucoside dimer (*5*) has also been established.

Two mechanisms have been postulated for direct reaction between anthocyanins and flavanols, leading, respectively, to tannin−anthocyanin ($T-A^+$) and anthocyanin−tannin (A^+-T) adducts.

In the formation of A^+-T (**Figure 1**), the anthocyanin is in the flavylium form (A^+) and acts as an electrophile. The hydroxyl groups in C5 and C7 have a mesomer effect and confer on the flavanol a nucleophilic character in C-6 or C-8. Nucleophilic addition of the flavanol onto the flavylium cation leads to the colorless flavene (A−T), which can either be oxidized to the red flavylium (A^+-T) and then to a xanthylium salt (*1*, *6*, *7*) or proceed to a colorless cyclic condensation product with an A type bond [A-(4−8, 2-O-7)-T]. The latter has recently been detected in wine and identified in model solution in our laboratory (*8*).

In the formation of $T-A^+$ (**Figure 2**), proanthocyanidins (T−T) are affected by acid-catalyzed cleavage of their interflavanic bond, releasing the intermediate carbocation T^+ (*9*), which acts as an electrophile, whereas the anthocyanin, in its hydrated hemiketal form (AOH), acts as a nucleophile (*10*). This yields the colorless dimer (T−AOH), which dehydrates to the red flavylium form ($T-A^+$).

Both reactions are expected to be pH dependent as the proportion of cationic forms (A^+ and T^+) should increase with acidity.

The purpose of this present work was to study direct reactions using model solutions to elucidate the mechanisms involved in these reactions, characterize eventual reaction products, and evaluate their formation kinetics and ability to occur in wine. Malvidin 3-*O*-glucoside (Mv3glc), the major anthocyanin in grapes, and procyanidin dimer Ec-EcG, one of the main procyanidin dimers in grape seeds, were used for this study. Selection of the latter was further justified by its particular structure in which the upper and lower units are different and thus can be distinguished in reaction products. The influence

* Corresponding author (e-mail salas@ensam.inra.fr; telephone 33 4 99 61 24 84; fax 33 4 99 61 26 83).

10.1021/jf0345402 CCC: $25.00
Published on Web 11/27/2003

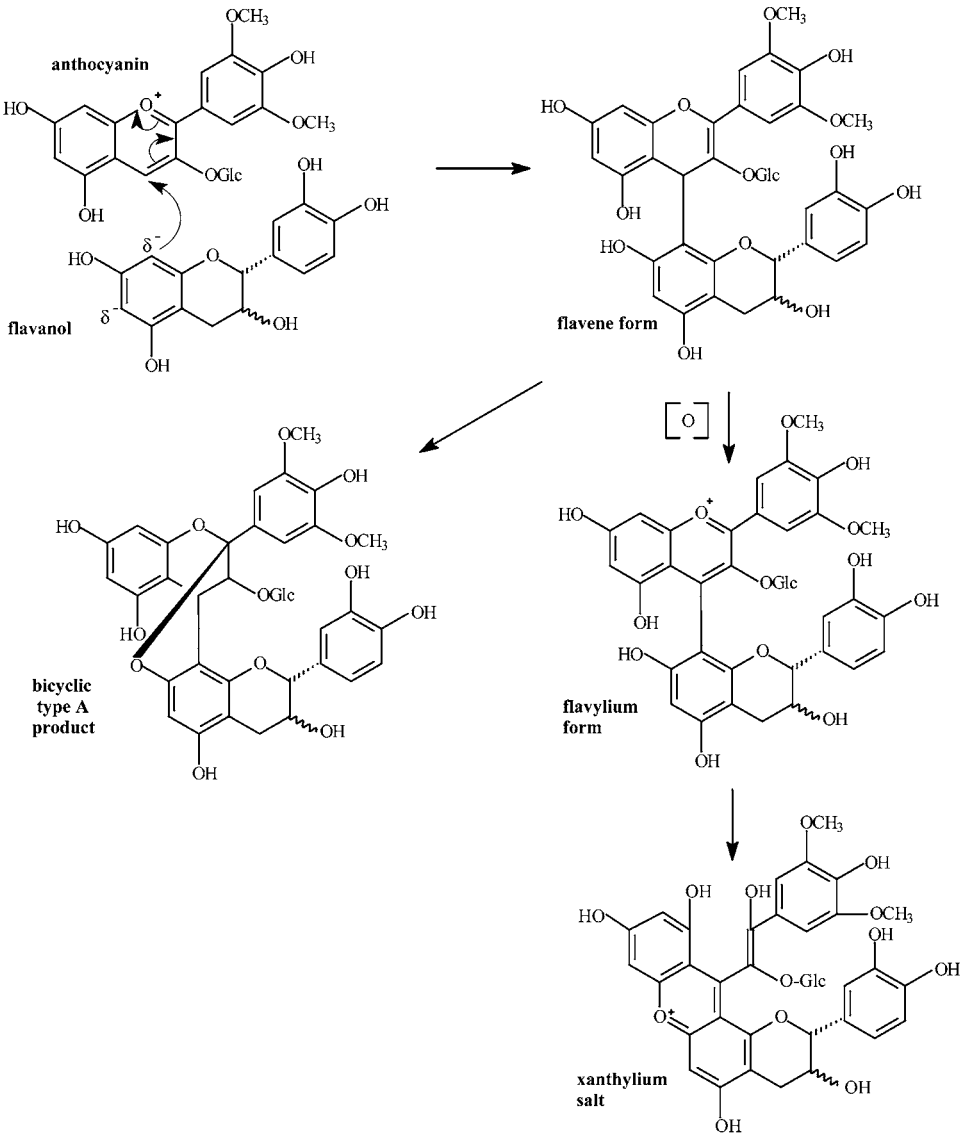

Figure 1. Mechanism of anthocyanin–tannin (A^+–T) formation.

of pH on anthocyanin and tannin reactions was also investigated, by comparing two pH values, 2.0 and 3.8. The former was chosen to favor acidic cleavage of the interflavanic bond and reactions involving the flavylium cation. The latter was selected as it is a typical pH value encountered in red wine.

MATERIALS AND METHODS

Materials. Organic solvents (HPLC grade) and phenylmethanethiol were purchased from Merck (Darmstadt, Germany) and Fluka (Buchs, Switzerland), respectively. Sodium metabisulfite was purchased from Prolabo (Fontenay s/Bois, France), and syringic acid and ammonium formate were from Sigma-Aldrich (Steinheim, Germany).

Isolation and Purification of Malvidin 3-*O*-glucoside and Ec-EcG Dimer. Mv3glc was extracted from grapes and purified in our laboratory as described by Sarni (*11*). The identity and purity of Mv3glc were checked by mass spectrometry and HPLC. Mv3glc was quantified from the area of its peak at 520 nm by HPLC using multiple-point calibration with external standard of commercial Mv3glc (Extrasynthése, Genay, France). Mv3glc was 90% pure, the other 10% corresponding to other anthocyanins, namely, peonidin 3-*O*-glucoside, malvidin 3,5-di-*O*-glucoside, and malvidin 3-*O*-acetylglucoside.

Procyanidin dimer Ec-EcG [B2 3′OG, (−)-epicatechin-(4β-8)-(−)-epicatechin 3-*O*-gallate] was purified by semipreparative HPLC from a grape seed fraction obtained in our laboratory as described by Ricardo da Silva (*12*).

Semipreparative HPLC. Semipreparative HPLC was performed using a Gilson system including a 305 master and a 306 slave pump, an 807 manometric module, an 811B dynamic mixer, a 7725 Rheodyne valve injector, and an 875 UV−visible Jasco detector set at 280 nm. The column was a reversed-phase Lichrospher 100 RP18 (5 μm packing, 125 × 22 mm). Elution conditions were as follows: 7 mL/min flow rate; temperature, 30 °C; solvent A, water/acetic acid (98:2, v/v); solvent B, methanol/solvent A (80:20, v/v); elution from 5 to 15% B in 10 min, from 15 to 22.5% B in 10 min, and from 22.5 to 80% B in 2 min, followed by washing and re-equilibration of the column. The isolated compound was lyophilized and used for further experiments. The identity and purity of the compound were checked by HPLC, thiolysis, and mass spectrometry. Ec-EcG was quantified from the area of its peak at 280 nm by HPLC using multiple-point calibration with an external standard of a previously isolated and characterized Ec-EcG dimer. The Ec-EcG dimer obtained had a purity of 90% as estimated by HPLC before and after thiolysis.

Model Solutions. *Solutions Containing Mv3glc and Ec-EcG.* Incubations were carried out at pH 2.0 and 3.8. The pH 2.0 solution was obtained in 5% formic acid adjusted by the addition of a 20% ammonia solution. The pH 3.8 solution was obtained in 20 mM ammonium formate solution adjusted by the addition of a 20% formic acid solution. For each pH condition, polyphenols were dissolved in the corresponding medium in order to obtain final concentrations of 1.4 mM for Mv3glc and 0.7 mM for Ec-EcG. The reaction was initiated by mixing the two polyphenol solutions. Each solution was distributed

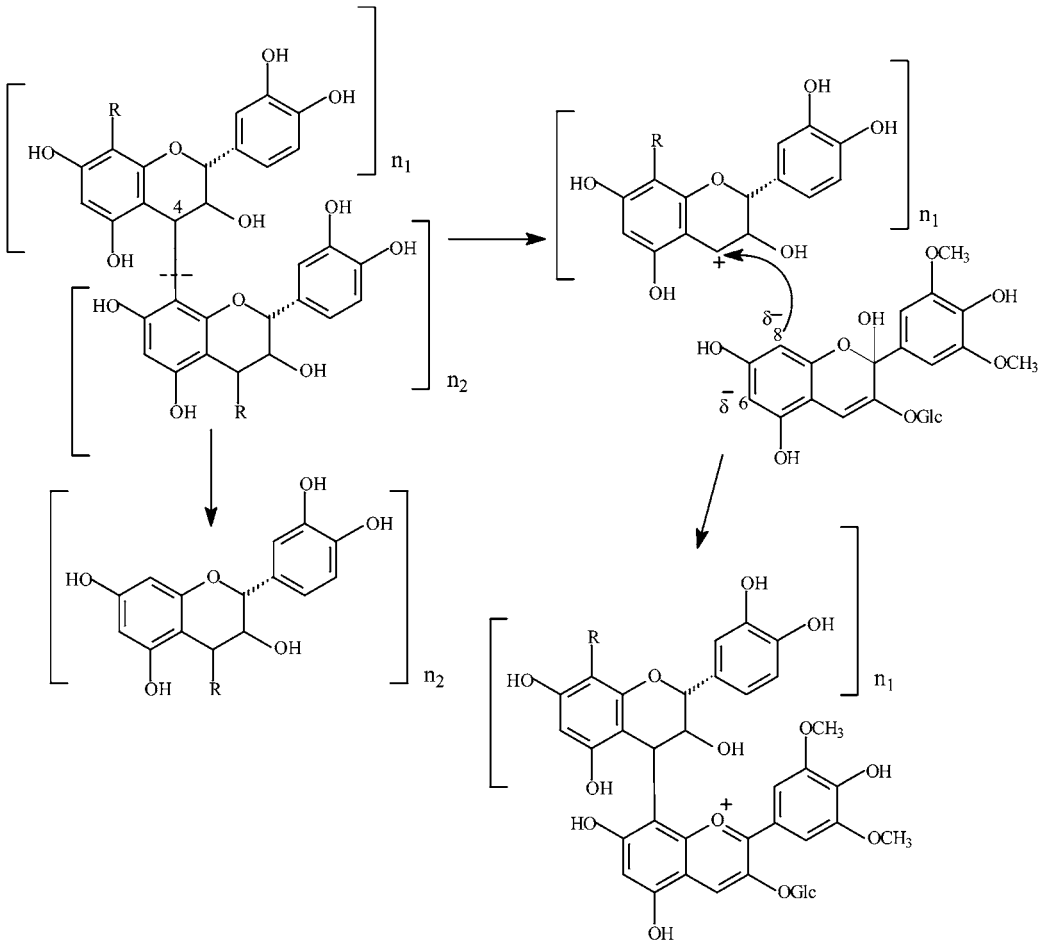

Figure 2. Mechanism of tannin–anthocyanin ($T–A^+$) formation.

in aliquots of 0.5 mL for each point of the kinetics (0, 6, 14, 24, 31, 45, and 64 days). Each 1 mL screw-cap vial was purged with argon and incubated at 30 °C in the dark.

Control solutions containing Mv3glc or Ec-EcG alone at the concentration used in mixture model solutions were incubated under the same conditions. All samples were prepared in triplicate.

HPLC-DAD. HPLC-DAD analyses were performed using a Waters 2690 system equipped with an autosampler system, a Waters 996 photodiode array detector, and Millenium 32 chromatography manager software (Milford, MA). Separation was achieved on a Lichrospher 100-RP18 column (5 μm packing, 250 mm × 2 mm i.d.) (Merck) protected with a guard column of the same material (Merck). The elution conditions were as follows: 0.250 mL/min flow rate; oven temperature, 30 °C; solvent A, water/formic acid (95:5, v/v); solvent B, acetonitrile/solvent A (80:20, v/v), elution began isocratically with 3% B for 7 min and was continued with linear gradients from 3 to 20% B in 15 min, from 20 to 30% B in 8 min, from 30 to 40% B in 10 min, from 40 to 50% B in 5 min, and from 50 to 80% B in 5 min, followed by washing and re-equilibration of the column. UV−vis spectra were recorded from 220 to 600 nm, and peak areas were measured at 280 and 520 nm.

HPLC—Electrospray Ionization (ESI)/MS. MS analyses and fragmentation experiments were performed on a ThermoFinnigan LCQ Advantage (San Jose, CA) mass spectrometer (MS) equipped with an ESI source and an ion trap mass analyzer, which were controlled by the LCQ navigator software. The mass spectrometer was operated in the positive and negative ion modes in the range of *m*/*z* 150−2000 and under the following conditions: source voltage, 4.5 kV; capillary voltage, 23.5 V; capillary temperature, 250 °C; collision energy for fragmentation, 25% for MS^2, 30% for MS^3, and 35% for MS^4. Chromatographic separation was achieved using a Waters 2690 system equipped with an autosampler system, a Waters 996 photodiode array detector, and Millenium 32 chromatography manager software. The column was a Lichrospher 100-RP18 (5 μm packing, 250 mm × 2 mm i.d.) protected with a guard column of the same material (Merck). The elution conditions were as follows: 0.250 mL/min flow rate; oven temperature, 30 °C; solvent A, water/formic acid (95:5, v/v); solvent B, acetonitrile/solvent A (80:20, v/v), elution began isocratically with 2% B for 7 min, continued with linear gradients from 2 to 20% B in 15 min, from 20 to 30% B in 8 min, from 30 to 40% B in 10 min, from 40 to 50% B in 5 min, and from 50 to 80% B in 5 min, followed by washing and re-equilibration of the column.

Thiolysis Conditions. One hundred microliters from each aliquot was taken to dryness under a nitrogen current and redissolved in 100 μL of methanol, and an equal volume of thiolytic reagent (toluene-α-thiol 5% in methanol containing 0.2 M HCl) was added. After sealing, the mixture was shaken and heated at 90 °C for 2 min. The thiolyzed solutions were then analyzed by LC-MS as described above.

Color Measurements. Absorbance measurements were performed with a SAFAS UV mc^2 spectrophotometer, with a 10 mm cell width, and were corrected for any dilution. Absorbance values were determined both at pH 2.0 and at pH 3.8 for all sets of solutions. Changing the pH from 2.0 to 3.8 was done to determine if the pigments that were formed at pH 2.0 remained colored at pH 3.8. Conversely, the pH was changed from 3.8 to 2.0 to estimate the amount of colorless anthocyanin adducts yielding to the colored flavylium forms under acidic conditions. pH changes were achieved by dilution with the buffer of the other pH or by adjusting the pH by addition of a 20% formic acid solution or a 20% ammonia solution. Absorbance measurements were performed 12 h later to ensure that the hydration equilibrium was reached.

Sulfite bleaching experiments were performed on the pH 3.8 solutions by adding 15 μL of a 1 M sodium metabisulfite solution. This bleaching is caused by the addition of hydrogen sulfite to the C-ring of the flavylium cation, generating a colorless hydrogen sulfite adduct (*13*, *14*). This process is reversible in acidic medium; therefore,

Table 1. Rate Constants of Mv3glc and Ec-EcG Disappearance

	$k = -\Delta \text{ Ln } C/\Delta T$ (days^{-1})	R^2
pH 2		
Mv3glc	0.0153	0.8478
Ec-EcG	0.0251	0.9217
Mv3glc control	0.0076	0.7925
Ec-EcG control	0.025	0.9612
pH 3.8		
Mv3glc	0.0639	0.9866
Ec-EcG	0.0456	0.9962
Mv3glc control	0.0294	0.7685
Ec-EcG control	0.0586	0.9664

to perform the sulfite bleaching experiments, the solutions at pH 2.0 must be changed to pH 3.8.

Absorbance measurements were done from 250 to 700 nm. Values at 280, 420, 520, and 620 were taken from the UV−visible spectra. After sulfite bleaching, the measurements were repeated and the absorbance value at 520 nm was taken from the spectra.

RESULTS AND DISCUSSION

Reaction Kinetics. Compositional changes were monitored by HPLC-DAD/MS. The disappearance of Mv3glc and Ec-EcG was modeled through first-order kinetics for each solution. The observed reaction rate constants (k) were determined using linear regression to plot the ln of the concentration at different time intervals (after 6, 14, 24, 31, 45, and 64 days) (**Table 1**). The disappearance of both species was much faster at pH 3.8 than at pH 2.0, meaning, on the one hand, that the hemiketal form of Mv3glc is less stable than its flavylium form, and, on the other hand, that reactions involving acid-catalyzed cleavage of the interflavanic bond are not predominant. Mv3glc disappeared 2 times more rapidly in the presence of Ec-EcG at both pH values, suggesting that Mv3glc reacts with Ec-EcG. The disappearance of Ec-EcG was slightly affected by the presence of Mv3glc at pH 3.8, but not at pH 2. The difference of k values for Ec-EcG at pH 3.8 (between control and mixture solutions) suggests that Mv3glc protects Ec-EcG from degradation.

These values show that there are other reactions besides the A^+-T and $T-A^+$ studied mechanisms. These unknown mechanisms are predominant at pH 3.8.

Monitoring of the Formation of Reaction Products by HPLC-DAD/MS. *Ec-EcG Solutions.* Changes in control solutions of Ec-EcG were monitored during a 64-day incubation period at pH 2.0 and 3.8. An HPLC profile at 280 nm at $t = 0$ and after 31 days of incubation is shown in **Figure 3**.

At pH 2.0, the appearance of a peak eluting at 27.09 min with a mass signal at m/z 441 (epicatechin gallate) indicated that the acidic cleavage of the Ec-EcG dimer had taken place. Monogalloylated trimers (m/z 1017), monogalloylated tetramers (m/z 1305), and monogalloylated pentamers (m/z 1593) were detected in the negative ion mode. These compounds result from the nucleophilic addition of Ec-EcG, $(Ec)_2$-EcG, and $(Ec)_3$-EcG, respectively, to the intermediate carbocation Ec^+, formed during cleavage of Ec-EcG, as described earlier (*9*, *15*). After a 6-day incubation period, the amount of EcG released was half the Ec-EcG consumed, as was to be expected from the following reaction:

$$2\text{Ec-EcG} \rightarrow \text{Ec}^+ + \text{EcG} + \text{Ec-EcG} \rightarrow \text{EcG} + \text{Ec-Ec-EcG}$$

After a longer time of incubation, the yield of EcG formed decreased, meaning that other reactions took place simultaneously.

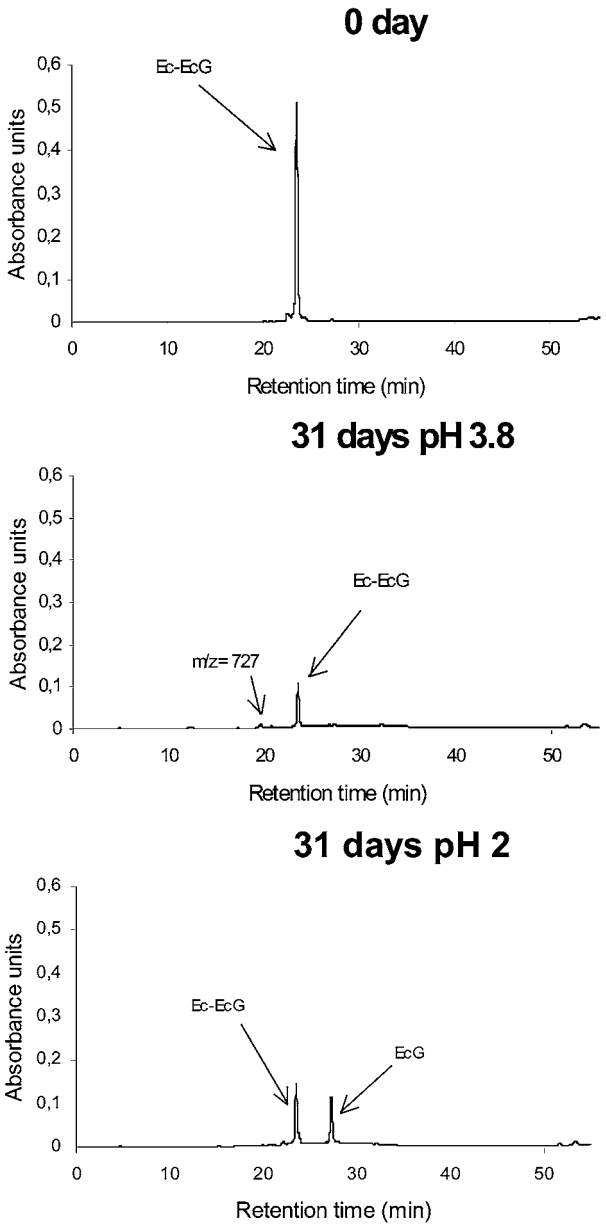

Figure 3. HPLC profile at 280 nm of the solution containing Ec-EcG at pH 2.0 and 3.8 at $t = 0$ days and after 31 days of incubation.

At pH 3.8, although the disappearance of Ec-EcG was faster than at pH 2.0, none of the monogalloylated oligomeric products observed in the pH 2.0 solution were detected, indicating that acid-catalyzed C−C bond breaking and bond-making processes did not take place or yielded different products from those observed at pH 2.0.

A peak eluting at 19.61 min and showing a mass signal at m/z 727, in the positive ion mode, and a $\lambda_{max} = 281.7$ nm appeared after 6 days of incubation and remained stable throughout the incubation period. Its mass value at m/z 727 suggests that it may be an oxidation product of Ec-EcG, similar to that obtained by autoxidation of procyanidin dimer B2 (*16*). The same peak was present at pH 2.0, but unlike the peak obtained at pH 3.8, it was smaller and disappeared after 2 weeks.

Thiolysis yield was inferior to the one obtained at pH 2.0, suggesting that other type of linkages have been formed which cannot be cleaved by thiolysis conditions.

An unresolved hump accumulated in both solutions. It was 3 times bigger for pH 2.0 than for pH 3.8, although larger amounts of unreacted Ec-EcG remained in the former solution.

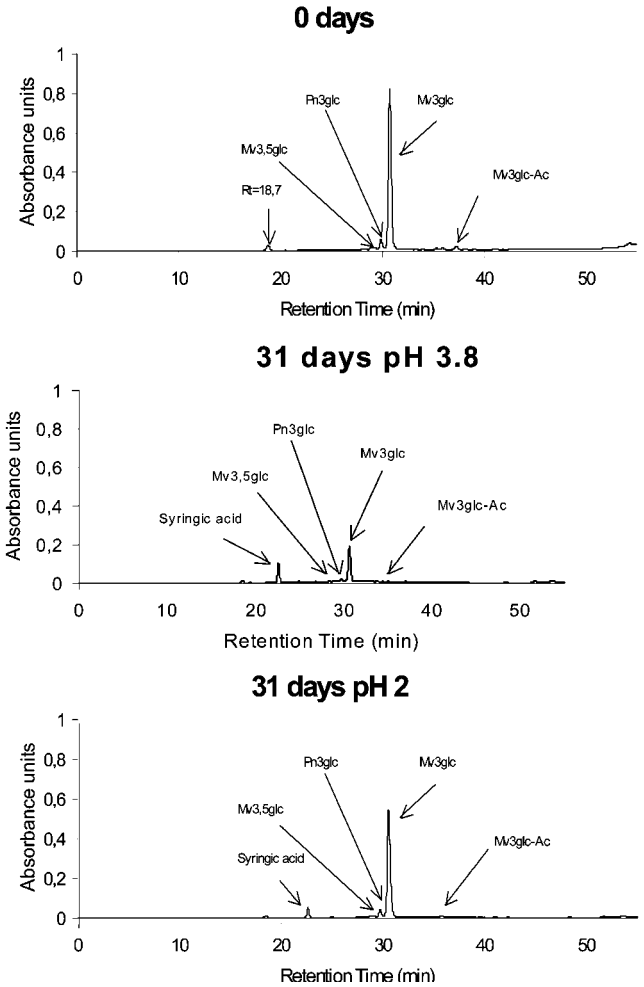

Figure 4. HPLC profile at 280 nm of the solution containing Mv3glc at pH 2.0 and 3.8 at $t = 0$ days and after 31 days of incubation.

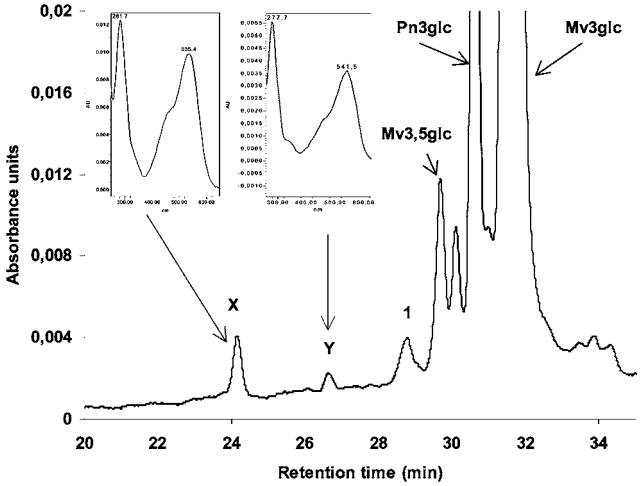

Figure 5. HPLC profile at 520 nm of the solution containing Mv3glc and Ec-EcG at pH 2.0 after 24 days of incubation.

Mv3glc Solutions. Changes in control solutions of Mv3glc were monitored at pH 2.0 and 3.8 for 64 days of incubation. An HPLC profile at 280 nm at $t = 0$ and after 31 days of incubation is shown in **Figure 4**.

At $t = 0$ an unknown compound (retention time of 18.7 min) with $\lambda_{max} = 291$ nm, which did not respond in MS and could not be interpreted, was also present.

Disappearance of Mv3glc was almost total after 64 days of incubation at pH 3.8. The major peak formed at pH 3.8 did not respond in MS. It was tentatively identified as syringic acid (eluting at 22.30 min) on the basis of its retention time and its UV spectrum, after co-injection with a reference compound. Formation of syringic acid results from cleavage of the heterocycle of the Mv chalcone form, which is in equilibrium with the hemiketal form (*17*), leading to syringic acid (from the B ring) and 2,4,6-trihydroxybenzaldehyde (from the A ring) (*18*).

At pH 3.8, the hydrated form of Mv3glc and of its aglycon were observed, respectively, at *m/z* 511 and 349 (eluting at 28.35 min). The aglycon is more sensitive to cleavage of the heterocycle leading to syringic acid than the glucoside. Additional compounds eluting at 31.72 and 33.20 min, probably corresponding to Mv3glc-Mv3glcOH (*m/z* 1001) and to the same adduct with one of the anthocyanins in its aglycon form (*m/z* 839), respectively, were also observed in trace amounts.

These adducts result from nucleophilic addition of one anthocyanin in its hydrated hemiketal form onto the other in the flavylium form, by a mechanism analogous to the formation of A^+-T, confirming that, at pH 3.8, anthocyanins react simultaneously as nucleophilic and as electrophilic agents.

At pH 2.0, in the control solution, during the first 2 weeks, the same peaks (*m/z* 511, 349, 839, 1001) were observed, but after 31 days, they were not present anymore.

The concentration of syringic acid was lower at pH 2.0 than at pH 3.8 but corresponded to ~15% of the Mv3glc consumed in both solutions after 64 days of incubation.

Solutions Containing both Mv3glc and Ec-EcG. In addition to Ecg, Ec-Ec-Ecg, and syringic acid, arising from the degradation of Ec-EcG and Mv3glc, a new compound (**X**) gradually accumulated until 24 days of incubation in the solution containing Mv3glc and Ec-EcG at pH 2.0 (**Figure 5**) and decreased afterward. This compound, showing a mass signal at *m/z* 781, in the positive ion mode, may correspond to the flavylium form of Ec-Mv3glc and was coeluted with Ec-EcG and therefore not visible at 280 nm. Its λ_{max} was at 535 nm (**Figure 5**). Its MS/MS fragmentation (**Figure 6**) gave two signals at *m/z* 763 and 619, which correspond, respectively, to the loss of a water molecule ($[M - 18]^+$), as described by Friedrich (*19*), and to loss of the anthocyanin glucose moiety ($[M - 162]^+$). MS^3 fragmentation of the ion at *m/z* 619 (**Figure 6**) gave four ions detected at *m/z* 601, 493, 467, and 373. The ion at *m/z* 601 corresponds to the loss of a water molecule ($[M - 18]^+$). The ion at *m/z* 493 ($[M - 126]^+$) can be interpreted as resulting from the loss of fragment $C_6H_6O_3$ (A ring). This fragmentation scheme indicates that the flavanol is the upper unit and the anthocyanin is the lower unit, because the fragment ion at *m/z* 493 (−126 amu) cannot arise from the anthocyanin A-ring and, according to Friedrich (*19*), it is specific of the upper unit of dimers. The ion at *m/z* 467 ($[M - 152]^+$) results from the retro-Diels–Alder decomposition (RDA) of the flavanol unit and provides no information on its position in the dimer. The ion at *m/z* 373 was shown to come directly from the ion at *m/z* 619 as it was not obtained by fragmentation of the other two ions at *m/z* 467 and 493; however, the ion at *m/z* 373 could not be interpreted. Nevertheless, the fragmentation pattern is in agreement with the postulated Ec-Mv3glc structure, which arises from nucleophilic addition of Mv3glc onto the carbocation Ec^+, issued from the acidic cleavage of Ec-EcG.

Another new compound (**Figure 5**, compound **Y**), with a mass signal at *m/z* 1069, in the positive ion mode, may correspond to the flavylium form of Ec-Ec-Mv3glc. The presence of the trimer (Ec-Ec-Mv3glc) is another argument in favor of the postulated mechanism leading to $T-A^+$ adducts.

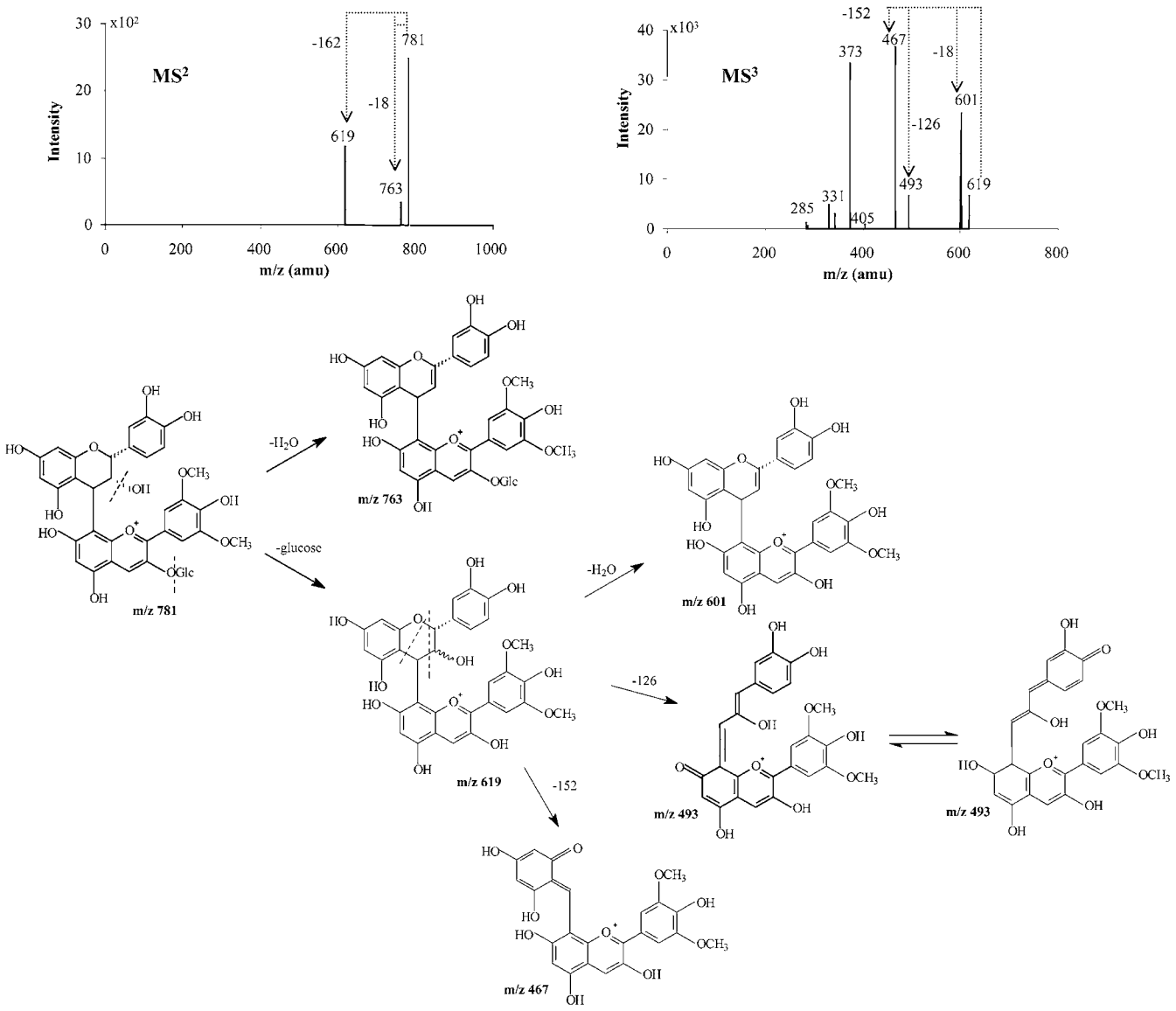

Figure 6. MS^2 and MS^3 analyses of the Ec-Mv3glc molecular ion (*m/z* 781).

Detection of these species (*m/z* 781 and 1069) indicates that, even at pH 2, the proportion of Mv3glc under the hemiketal form is sufficient to enable their formation. Trapping of the hemiketal form in this reaction should further displace the hydration equilibrium of Mv3glc under its flavylium form to the hydrated hemiketal form.

Another peak eluting at 28.7 min (**Figure 5**, compound **1**), with a $\lambda_{max} = 522$ nm and a mass signal at *m/z* 817, was coeluted with a signal at *m/z* 511 corresponding to the Mv3glc in its hydrated hemiketal form or in the isomeric yellow chalcone form. Interpretation of the signal at *m/z* 817 was not achieved.

Incubation of Mv3glc and Ec-EcG at pH 3.8 did not give rise to compound **X** or **Y** but yielded another product (**Z**) with a mass signal at *m/z* 1221, in the positive ion mode, and a $\lambda_{max} = 541$ nm (**Figure 7**), which was not found in the control solution of Mv3glc at pH 3.8 and corresponds probably to $Mv3glc^+$-Ec-EcG. This product gradually accumulated until 14 days of incubation and disappeared afterward. It is expected to result from nucleophilic addition of Ec-EcG onto Mv3glc in its flavylium form.

Ion extraction at *m/z* 1221 allowed two compounds to be distinguished within the **Z** peak, eluting at 21.25 and 22.5 min,

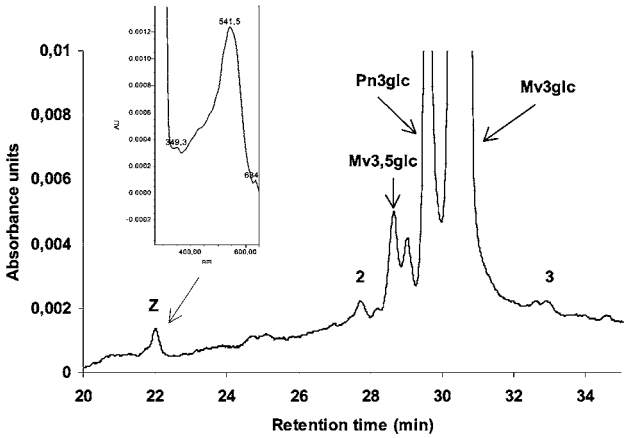

Figure 7. HPLC profile at 520 nm of the solution containing Mv3glc and Ec-EcG at pH 3.8 after 14 days of incubation.

respectively. MS/MS analysis was performed for each compound. MS/MS analysis of the signals at *m/z* 1221 (**Figure 8**) gave the same two fragments detected at *m/z* 1059 and 1203, which correspond, respectively, to the loss of the glucose moiety

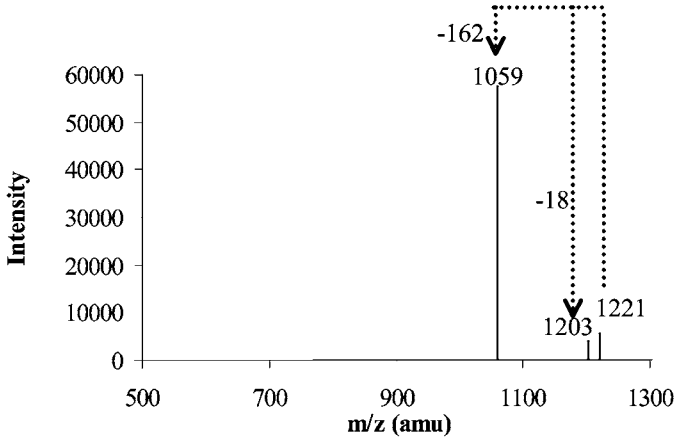

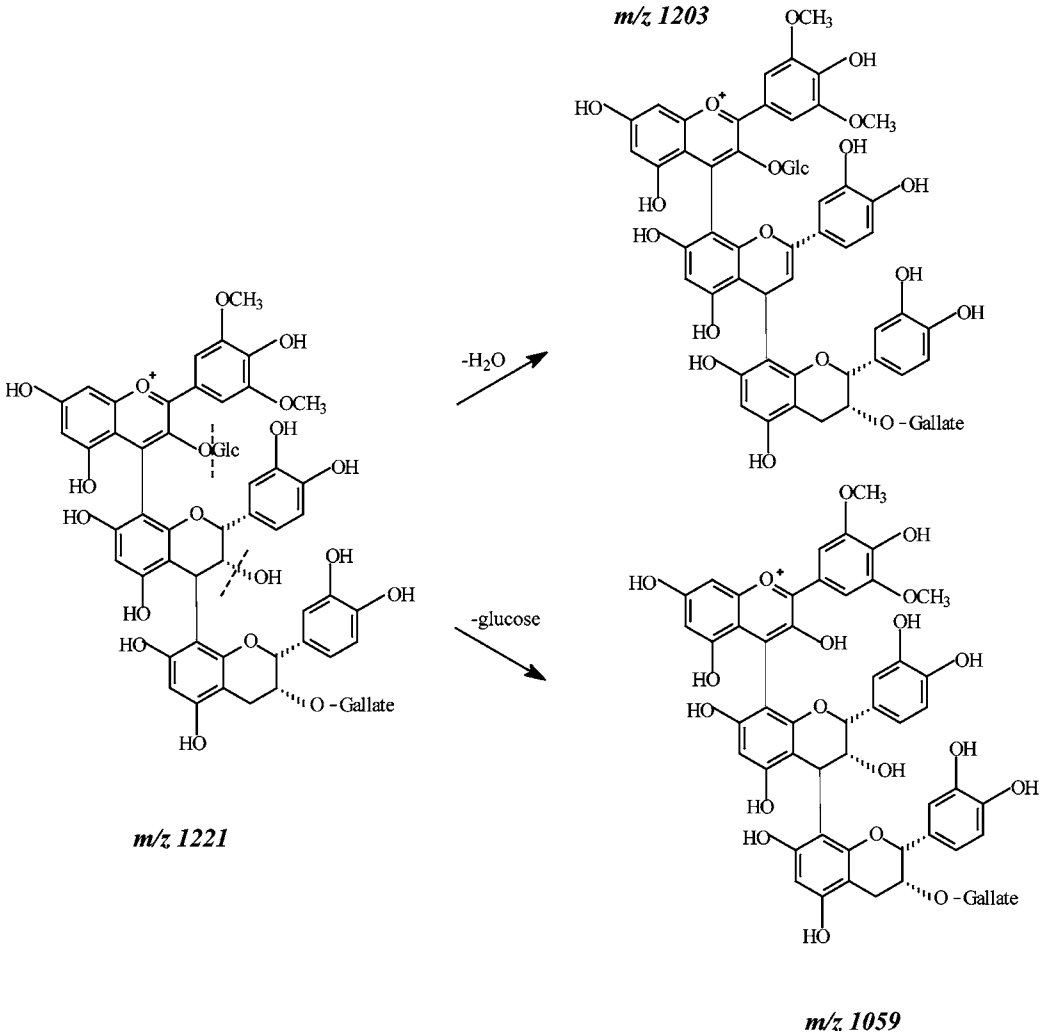

Figure 8. MS^2 analysis of the Mv3glc-Ec-EcG molecular ion (*m/z* 1221).

($[M - 162]^+$), coming from the anthocyanin unit, and the loss of a water molecule ($[M - 18]^+$). MS^3 of the ion at *m/z* 1059 (**Figure 9**) yielded different fragmentation patterns for the two compounds. That of the most abundant (retention time = 22.5 min), gave four ions detected at *m/z* 1041, 617, 907, and 755. The ion at *m/z* 1041 corresponds to the loss of a water molecule ($[M - 18]^+$) and that at *m/z* 907 to the loss of the gallate unit ($[M - 152]^+$). The ion at *m/z* 617 results from the loss of epicatechin gallate, releasing Mv-Ec ($[M - 442]^+$) in the quinonoidal form as described by Barofsky (*20*). This fragmentation scheme indicates that epicatechin gallate is the lower unit, in agreement with the proposed structure, $Mv3glc^+$-Ec-EcG. The ion at *m/z* 755 comes from the loss of 152 amu, which is interpreted by the RDA on any of the two flavanol units.

MS^3 of the ion at *m/z* 1059 (**Figure 10**) obtained after fragmentation of the other compound detected at *m/z* 1221 gave an ion at *m/z* 771, which corresponds to the loss of an

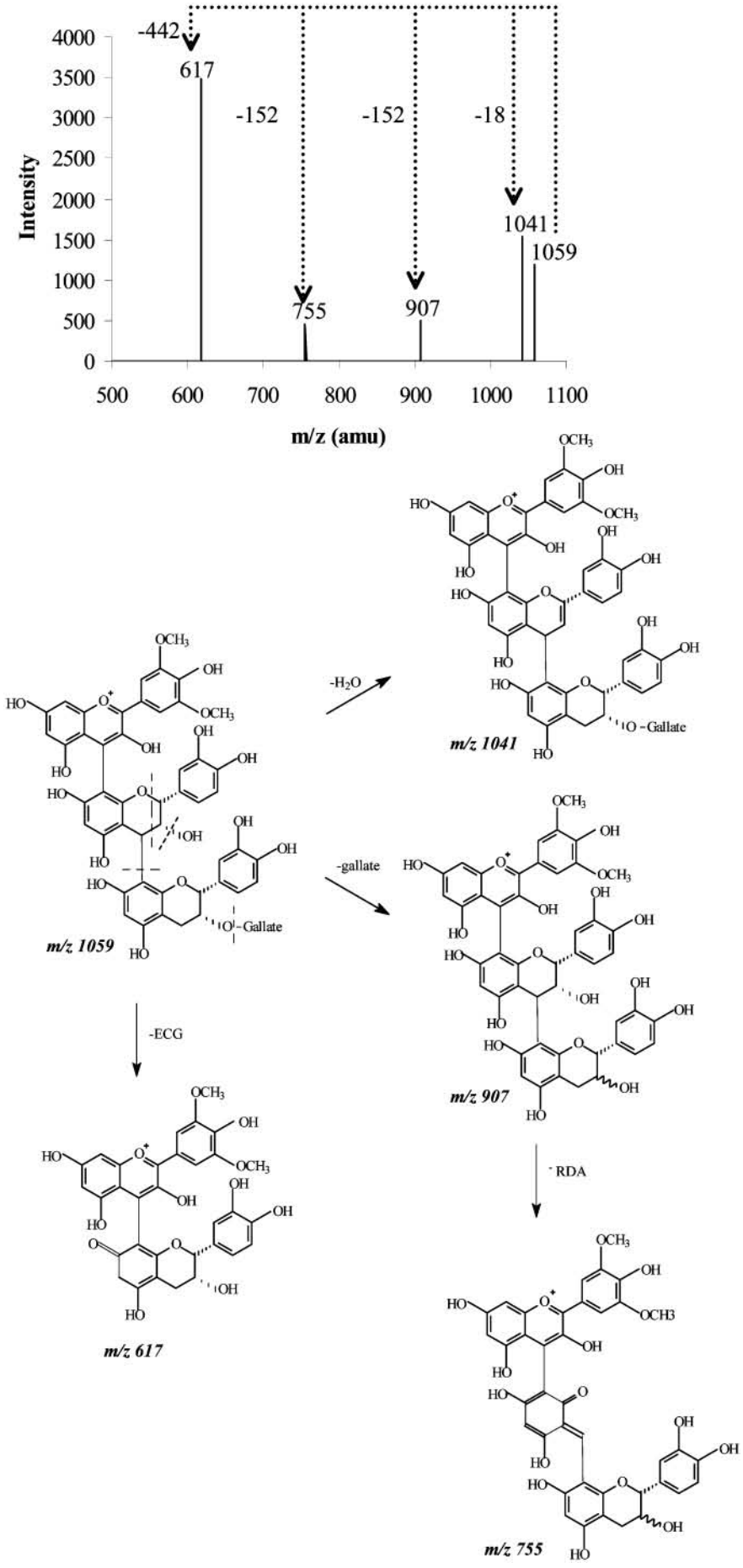

Figure 9. MS^3 analysis of the fragment ion at *m/z* 1059.

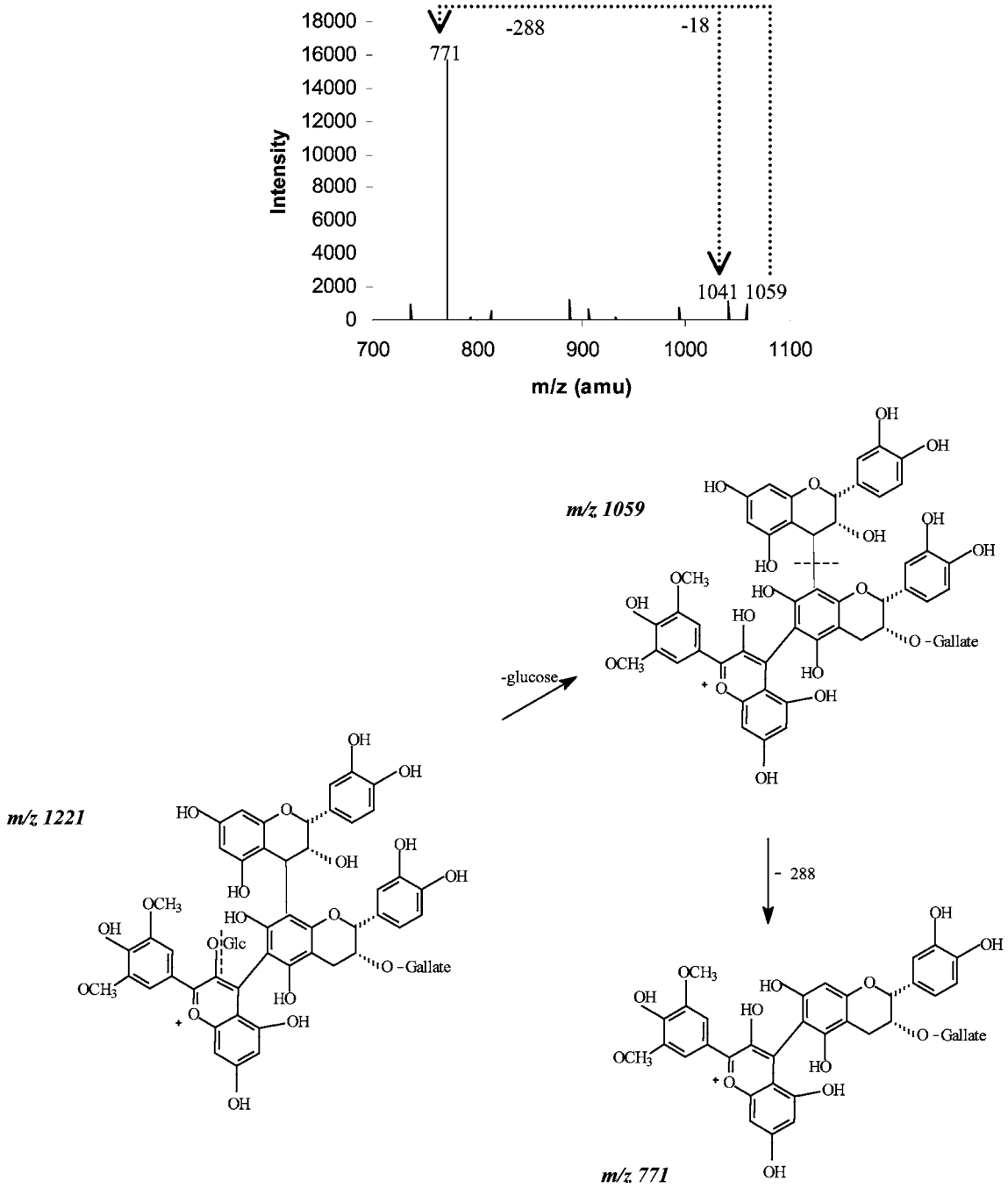

Figure 10. Fragmentation pattern of the (Ec-(4–8)-(Mv3glc-(4–6)-EcG) molecular ion and MS^3 analysis of the fragment ion at *m/z* 1059.

epicatechin unit ($[M - 288]^+$) in the quinonoidal form (*20*) in the upper position. This fragmentation scheme thus does not fit with the proposed $Mv3glc^+$-Ec-EcG structure and suggests that $Mv3glc^+$ is also linked to the EcG moiety, presumably through an $Mv3glc^+$-(4−6)-EcG linkage [Ec-(4−8)-($Mv3glc^+$-(4−6)-EcG].

MS analysis of the peak eluting at 27.9 min (**Figure 7**, compound **2**) showed mass signals at *m/z* 511, 493, 349, 331, and 857. The first four signals correspond to Mv3glc in its hydrated form and to fragments generated by loss of water and/or glucose. The signal at *m/z* 857 could not be interpreted but is probably responsible for the absorbance in the visible region. The anthocyanin dimer present in the Mv3glc solution incubated at pH 3.8 was also detected, but only as its aglycon form (*m/z* 839), eluting at 33.35 min (**Figure 7**, compound **3**).

Analysis of Reaction Media by Thiolysis. The reaction media containing Ec-EcG were also analyzed by HPLC after thiolysis. This method has been developed for the analysis of proanthocyanidins (*21*, *22*) but can also provide structural information on tannin−anthocyanin derivatives (*23*, *24*). Its relies upon acid-catalyzed depolymerization in the presence of toluene-α-thiol, used as a nucleophilic agent to trap the released T^+ carbocation. Analysis of the resulting solution then enables one to distinguish between the terminal units (substituted in C-6 or C-8 in the original structure), which are released as such, and the upper and intermediate units (substituted in the 4-position in the original structure), which yield the corresponding benzylthioether derivatives.

Thiolysis yields calculated from the initial quantity of Ec-EcG were 70% at $t = 0$, as usually obtained with pure

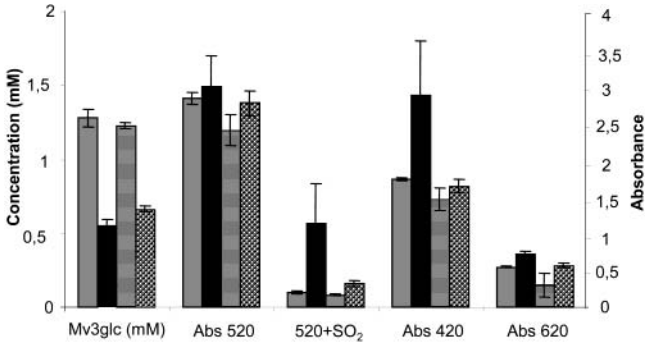

Figure 11. Concentration of Mv3glc in the solutions incubated at pH 2.0 and absorbance values measured after adjustment of the pH at 3.8. Bars represent, from left to right in each grouping, Ec-EcG+Mv3glc at $t = 0$, Ec-EcG+Mv3glc at $t = 64$ days, Mv3glc at $t = 0$, and Mv3glc at $t = 64$ days. Error bars = ± standard deviation, 95% confidence limits.

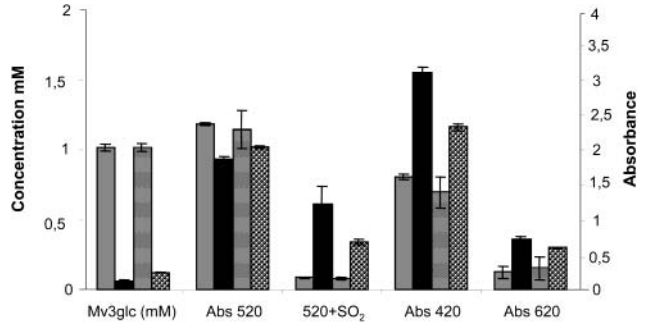

Figure 12. Concentration of Mv3glc in the solutions incubated at pH 3.8 and absorbance values measured at 3.8. Bars represent, from left to right in each grouping, Ec-EcG+Mv3glc at $t = 0$, Ec-EcG+Mv3glc at $t = 64$ days, Mv3glc at $t = 0$, and Mv3glc at $t = 64$ days. Error bars = ± standard deviation, 95% confidence limits.

procyanidins (*25*). They decreased to 16 and 2%, after 45 days of incubation at pH 2.0 and 3.8, respectively.

After thiolysis of the solutions incubated at pH 2.0, the ion at *m*/*z* 781 was still present, meaning that T−A^+ pigments are resistant or at least partly resistant to thiolysis. In fact, the occurrence of the flavylium moiety within these structures is expected to increase the resistance to acid-catalyzed cleavage as it cannot undergo the proton addition needed to initiate acidic cleavage. Such increased resistance has been demonstrated in the case of ethyl-linked flavanol−anthocyanin adducts (*26*).

In the solutions incubated at pH 3.8, the ion at *m*/*z* 1221, attributed to Mv3glc$^+$-Ec-EcG and Ec-(Mv3glc$^+$-EcG) as discussed above, was no longer detected after thiolysis. Two additional ions were detected at *m*/*z* 903 and 933, in the positive ion mode. They can be respectively interpreted as the benzylthioether derivative of Mv3glc$^+$-Ec, arising from thiolysis of Mv3glc$^+$-Ec-EcG, and as Mv3glc$^+$-EcG, which is the terminal unit of Ec-(Mv3glc$^+$-EcG), confirming the presence of both structures in the original solution.

The ions at *m*/*z* 839 and 1001 were still present after thiolysis.

Monitoring of Color Changes in the Solutions Containing Pigments. Absorbance measurements were carried out throughout the incubation period. Values measured at $t = 0$ and after 64 days of incubation at pH 2.0 and 3.8 are presented in **Figures 11** and **12**, respectively.

In the solutions incubated at pH 2.0, the absorbance at 520 nm was highly correlated with the amount of residual Mv3glc ($p = 0.91$ in the Mv3glc solution; $p = 0.94$ in the solution containing Mv3glc and Ec-EcG), indicating that Mv3glc was the major species contributing color in the acidic media. However, the absorbance values measured at 520 nm after adjustment of the pH at 3.8 in the pH 2.0 solutions (**Figure 11**) remained almost constant over the incubation period, whereas Mv3glc concentration decreased >60%. This means that the formation of new pigments compensated for the loss of Mv3glc. These pigments are apparently less susceptible to hydration than Mv3glc and mostly colored at pH 3.8, as shown in the case of ethyl-linked Mv3glc dimer (*28*). They also contributed to the absorbance at 420 and 620 nm and increased resistance to sulfite bleaching, especially in the solution containing Ec-EcG. Similar trends were observed in the solutions incubated at pH 3.8, but the absorbance values at 520 nm measured at pH 3.8 decreased slightly, whereas absorbances at 420 and 620 nm increased greatly. Absorbance values in the yellow region as well as color resistance to sulfite bleaching were also higher in the solutions incubated at pH 3.8 than in those incubated at pH 2.0, suggesting that different products were formed under the two pH conditions.

This increased resistance to sulfite bleaching may be explained by the major structures formed in the different media. In fact, A^+−T and A^+−AOH adducts are expected to be resistant toward sulfite and water addition, owing to the substitution of the anthocyanin C-ring, whereas T−A^+ adducts should not be unless they are stabilized by copigmentation as shown for the equivalent ethyl-linked derivatives (*27*, *28*).

Conclusion. The results obtained in this study show that anthocyanins are more stable at pH 2.0 than at pH 3.8 and react more rapidly in the presence of procyanidins. Direct reactions of anthocyanins and procyanidins leading to T−A^+ and A^+−T adducts were demonstrated. Formation of T−A^+ adducts appeared to be essentially limited by the rate of proanthocyanidin acid-catalyzed cleavage and was not observed at pH 3.8. However, it is expected to take place in the lower values of wine pH range because cleavage of proanthocyanidins has been shown to occur at pH 3.2 (*15*). In contrast, A^+−T species were detected only at the higher pH value. These adducts resulted from nucleophilic addition of the flavanol onto the electrophilic anthocyanin flavylium cation. However, the presence of Mv3glc-Mv3glcOH (A^+−AOH) indicated that anthocyanins react both as nucleophilic and as electrophilic species under these conditions. Further work to isolate and characterize T−A^+ and A^+−T derivatives and determine their color properties is under way.

ABBREVIATIONS USED

Mv3glc, malvidin 3-*O*-glucoside; Ec-EcG, procyanidin dimer epicatechin−epicatechin-3′-*O*-gallate; T−A^+, tannin−anthocyanin; A^+−T, anthocyanin−tannin; HPLC, high-performance liquid chromatography; ESI, electrospray ionization; MS, mass spectrometry; LC; liquid chromatography; DAD, diode array detector; ln, Napierian logarithm; *k*, observed reaction rate constant; *m*/*z*, mass/charge; EcG, epicatechin-3′-*O*-gallate; Ec, epicatechin; *t*, time; RDA, retro-Diels−Alder decomposition; t_R, retention time; Mv, malvidin; Ec-Mv3glc, epicatechin−malvidin 3-*O*-glucoside dimer; Ec-Ec-Mv3glc, epicatechin−epicatechin−malvidin 3-*O*-glucoside trimer; Mv3glc-Ec-EcG, malvidin 3-*O*-glucoside−epicatechin−epicatechin-3′-*O*-gallate trimer; Abs, absorbance; *C*, concentration.

ACKNOWLEDGMENT

We thank Sophie Remy-Tanneau for purifying Mv3glc.

LITERATURE CITED

(1) Somers, T. C. The polymeric nature of wine pigments. *Phytochemistry* **1971**, *10*, 2175−2186.

(2) Timberlake, C. F.; Bridle, P. Interactions between anthocyanins, phenolic compounds, and acetaldehyde and their significance in red wines. *Am. J. Enol. Vitic.* **1976**, *27*, 97−105.

(3) Dallas, C.; Ricardo-da-Silva, J. M.; Laureano, O. Products formed in model wine solutions involving anthocyanins, procyanidin B2 and acetaldehyde. *J. Agric. Food Chem.* **1996**, *44*, 2402−2407.

(4) Es-Safi, N.; Fulcrand, H.; Cheynier, V.; Moutounet, M.; Hmamouchi, M.; Essassi, E. M. Kinetic studies of acetaldehyde-induced condensation of flavan-3-ols and malvidin-3-glucoside in model solution systems. *JIEP 96* **1996**, 279−280.

(5) Atanasova, V.; Fulcrand, H.; Le Guerneve, C.; Cheynier, V.; Moutounet, M. Structure of a new dimeric acetaldehyde malvidin 3-glucoside condensation product. *Tetrahedron Lett.* **2002**, *43*, 6151−6153.

(6) Jurd, L. Review of polyphenol condensation reactions and their possible occurrence in the aging of wines. *Am. J. Enol. Vitic.* **1969**, *20*, 197−195.

(7) Liao, H.; Cai, Y.; Haslam, E. Polyphenol interactions. Anthocyanins: co-pigmentation and color changes in red wines. *J. Sci. Food Agric.* **1992**, *59*, 299−305.

(8) Remy-Tanneau, S.; Guerneve, C. L.; Meudec, E.; Cheyneir, V. Characterization of a colorless anthocyanin-flavan-3-ol dimer containing both carbon−carbon and ether interflavanoid linkages by NMR and mass spectrometries. *J. Agric. Food Chem.* **2003**, in press.

(9) Haslam, E. In vino veritas: oligomeric procyanidins and the ageing of red wines. *Phytochemistry* **1980**, *19*, 2577−2582.

(10) Ribéreau-Gayon, P. *The Anthocyanins of Grapes and Wines*; Academic Press: New York, 1982; pp 209−244.

(11) Sarni, P.; Fulcrand, H.; Souillol, V.; Souquet, J.-M.; Cheynier, V. Mechanisms of anthocyanin degradation in grape must-like model solutions. *J. Sci. Food Agric.* **1995**, *69*, 385−391.

(12) Ricardo da Silva, J. M.; Rigaud, J.; Cheynier, V.; Cheminat, A.; Moutounet, M. Procyanidin dimers and trimers from grape seeds. *Phytochemistry* **1991**, *30*, 1259−1264.

(13) Timberlake, C.; Bridle, P. Flavylium salts, anthocyanidins and anthocyanins. II. Reactions with sulphur dioxide. *J. Sci. Food Agric.* **1967**, *18*, 473−478.

(14) Berke, B.; Chèze, C.; Vercauteren, J.; Deffieux, G. Bisulfite addition to anthocyanins: revisited structures of colorless adducts. *Tetrahedron Lett.* **1998**, *39*, 5771−5774.

(15) Vidal, S.; Cartalade, D.; Souquet, J.; Fulcrand, H.; Cheynier, V. Changes in proanthocyanidin chain-length in wine-like model solutions. *J. Agric. Food Chem.* **2002**, *50*, 2261−2266.

(16) Zhu, Q.; Hammerstone, J.; Lazarus, S.; Schmitz, H.; Keen, C. Stabilizing effect of ascorbic acid on flavan-3-ols and dimeric procyanidins from cocoa. *J. Agric. Food Chem.* **2003**, *51*, 828−833.

(17) Brouillard, R.; Delaporte, B. Chemistry of anthocyanin pigments. 2. Kinetic and thermodynamic study of proton transfer, hydration, and tautomeric reactions of malvidin 3-glucoside. *J. Am. Chem. Soc.* **1977**, *99*, 8461−8468.

(18) Piffaut, B.; Kader, F.; Girardin, M.; Metche, M. Comparative degradation pathways of malvidin 3,5-diglucoside after enzymatic and thermal treatments. *Food Chem.* **1994**, *59*, 115−120.

(19) Friedrich, W.; Eberhardt, A.; Galensa, R. Investigation of proanthocyanidins by HPLC with electrospray ionization mass spectrometry. *Eur. Food Res. Technol.* **2000**, *211*, 56−64.

(20) Barofsky, D. FAB-MS applications in the elucidation of proanthocyanidin structure. In *Chemistry and Significance of Condensed Tannins*; Hemingway, R., Karchesy, J., Eds.; Plenum Press: New York, 1988; pp 175−195.

(21) Thompson, R. S.; Jacques, D.; EHaslam; Tanner, D. J. N. Plant proanthocyanidins. Part. I. Introduction: the isolation, structure, and distribution in nature of plant procyanidins. *J. Chem. Soc., Perkin Trans. 1* **1972**, 1387−1399.

(22) Rigaud, J.; Perez-Ilzarbe, X.; Ricardo da Silva, J. M.; Cheynier, V. Micro method for the identification of proanthocyanidin using thiolysis monitored by high-performance liquid chromatography. *J. Chromatogr.* **1991**, *540*, 401−405.

(23) Remy, S.; Fulcrand, H.; Labarbe, B.; Cheynier, V.; Moutounet, M. First confirmation in red wine of products resulting from direct anthocyanin-tannin reactions. *J. Sci. Food Agric.* **2000**, *80*, 745−751.

(24) Atanasova, V.; Fulcrand, H.; Cheynier, V.; Moutounet, M. Effect of oxygenation on polyphenol changes occurring in the course of wine making. *Anal. Chim. Acta* **2002**, *458*, 15−27.

(25) Cheynier, V.; Labarbe, B.; Moutounet, M. Estimation of procyanidin chain length. *Methods Enzymol.* **2001**, *335*, 82−94.

(26) Es-Safi, N.; Fulcrand, H.; Cheynier, V.; Moutounet, M. Studies on the acetaldehyde-induced condensation of (−)-epicatechin and malvidin 3-*O*-glucoside in a model solution system. *J. Agric. Food Chem.* **1999**, *47*, 2096−2102.

(27) Escribano-Bailon, T.; Alvarez-Garcia, M.; Rivas-Gonzalo, J. C.; Heredia, F. J.; Santos-Buelga, C. Color and stability of pigments derived from the acetaldehyde-mediated condensation between malvidin-3-*O*-glucoside and (+)-catechin. *J. Agric. Food Chem.* **2001**, *49*, 1213−1217.

(28) Atanasova, V. Réactions des composés phénoliques induites dans les vins rouges par la technique de micro-oxygénation. Caractérisation d'enouveaux produits de condensation des anthocyanes avec l'acétaldéhyde; ENSAM, 2003.

Received for review May 23, 2003. Revised manuscript received September 25, 2003. Accepted October 5, 2003. We thank the Consejo Nacional de Ciencia y Tecnologia (CONACYT, Mexico) for providing doctoral financing in a cooperation program with the Société Française d'Exportation des Ressources Educatives (SFERE, France). This work was also partly funded by the European Commission (QLRT-1999-00505).

JF0345402